

## Inversion-Recovery-Prepared Sliding Interleaved Cylinder (SLINCY) Imaging

Kie Tae Kwon<sup>1</sup>, Bob S Hu<sup>2</sup>, and Dwight G Nishimura<sup>1</sup>

<sup>1</sup>Electrical Engineering, Stanford University, Stanford, CA, United States, <sup>2</sup>Palo Alto Medical Foundation, Palo Alto, CA, United States

**Purpose:** A sliding interleaved cylinder (SLINCY) acquisition is a variation of a sliding interleaved  $k_y$  (SLINKY) [1] acquisition in which a 3D concentric cylinders trajectory [2] is used as the readout instead of a 3DFT sequence. Previously, SLINCY was incorporated into a non-contrast-enhanced (NCE) magnetization-prepared 3D SSFP sequence to improve artery-vein contrast in the lower extremities [3]. However, one of remaining issues for this approach is to suppress the long- $T_1$  fluids such as joint fluid or edema, which can otherwise hamper the depiction of arterial blood in the SSFP images due to their higher  $T_2/T_1$  ratios. In this work, we exploited the thin-slab-scan nature of SLINCY to efficiently add inversion-recovery (IR) [4] to suppress the fluids. **Methods:** SLINCY: The SLINCY acquisition consists of a series of overlapped thin slabs for volumetric coverage, with the increment of slab location equal to the resolution in the slab direction (Fig. 1a). For each thin slab, one of  $N$  interleaved subsets of concentric cylinders (Fig. 1a) is collected. Still, each slab is fully sampled in  $k_z$ , so slices can be reconstructed without aliasing in the  $z$  direction. Therefore, each slice can be reconstructed by combining partial data from  $N$  slabs that include the slice after 3D gridding.

IR-SLINKY: Figure 1b shows the timing diagram, which shows the array of preparations, i.e., IR, T2-preparation (T2-Prep) [5], and venous/fat saturation pulses that are applied before the SSFP cylinders readout. For the original SLINCY with no IR, only block B was repeated  $N_B$  times for each slab (Fig 1c). For the new IR-SLINKY, block A with selective IR and T2-Prep (to suppress the recovered muscle signal during IR) is added in front of block B. To prevent a substantial increase of scan time due to the recovery time ( $T_{recovery,A}$ ) and inversion delay (TI), two different IR schemes are considered. **1) IR scheme 1:** block A is applied to each slab, but the increment of slab location is adjusted in a way that the next slab is not overlapped with the current slab (Fig. 2a vs. Fig. 2b). This allows sufficient recovery of fluids without introducing an explicit recovery time. In addition, IR is prepared for the next slab instead of the current slab such that the duration for acquiring the current slab is used as TI for the next slab [6]. **2) IR scheme 2:** block A is applied to a group of overlapped slabs ( $N_{group}$ ), but the groups are selected from the superior/inferior side of the FOV in turn to allow sufficient recovery of fluids similar to IR scheme 1 (Fig. 2c). In each group, the first slab is chosen to be the one that collects the innermost (within each group) interleaved subsets of cylinders to efficiently capture the effect of fluid suppression. Unlike scheme 1, IR is applied to the current (not the next) group such that an explicit TI is used and the scan time is increased a bit longer.

Imaging Parameters: An *in vivo* study of the lower extremity on a healthy volunteer was performed on a GE Excite 1.5 T scanner with an extremity coil. Gradients for the SSFP version of the SLINCY acquisition were designed to provide isotropic resolution = 1.2 mm and FOV = 340×340×38.4 mm<sup>3</sup> for each slab. TE/TR = 3.7/7.4 ms, and flip angle = 60°. Each slab with  $N = 16$  consisted of  $N_B = 4$  segments with  $T_{recovery,B} = 100$  ms, which took 1.6 s without block A. 192 slabs were acquired to cover 21 cm in the S/I direction. For IR scheme 2,  $N_{group} = 4$  slabs were acquired per group with TI = 1.9 s. Total scan time was 5 min 20 s / 5 min 40 s / 6 min 30 s for No-IR / IR scheme 1 / IR scheme 2, respectively.

**Results:** Figure 3 shows axial (top) and coronal (bottom) MIP images of the lower extremities with (a) no IR, (b) IR scheme 1, and (c) IR scheme 2. Among these, IR scheme 2 provides a reasonable trade-off between fluid suppression (dashed arrows, dashed boxes) and arterial signal (solid arrows) by introducing an explicit TI with the expense of a longer scan time.

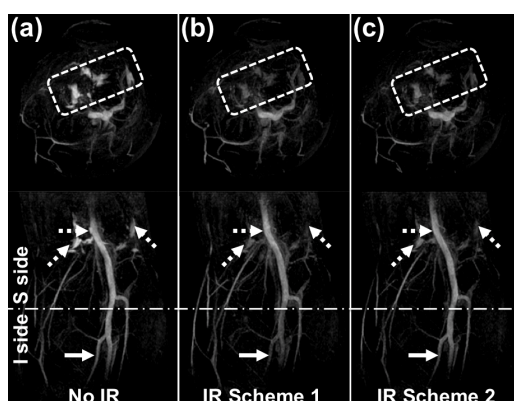


**Fig. 3.** Axial (top) and coronal (bottom) MIP (factor of two zero-padding) of the lower extremity with SLINCY. (a) No IR (b) IR scheme 1 (c) IR scheme 2. Among these, IR scheme 2 provides a reasonable trade-off between fluid suppression (dashed arrows, dashed boxes) and arterial signal (solid arrows).

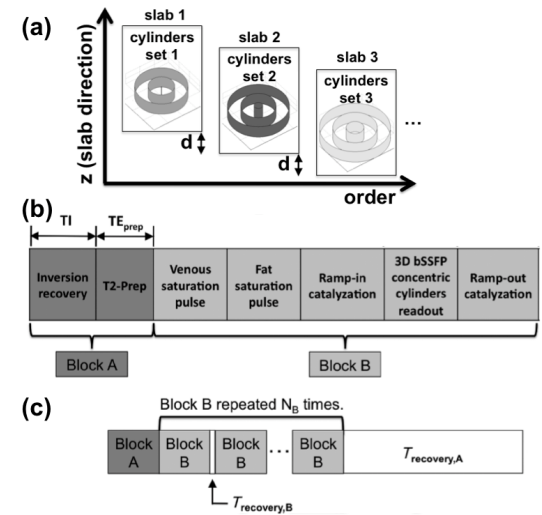


**Fig. 1.** (a) Data acquisition scheme of SLINCY. A partial set of cylinders is collected at each slab in an interleaved way, incremented by a distance  $d$  equal to the resolution in  $z$  for the subsequent slab. (b,c) The timing diagram within each slab.

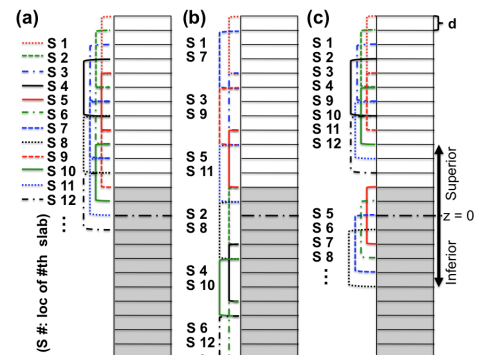


**Fig. 2.** Acquisition order of slabs (e.g., S1: 1<sup>st</sup> slab) for SLINCY with (a) No IR (b) IR scheme 1 (c) IR scheme 2. Both IR schemes apply selective IR to the superior/inferior half (white/gray areas) of the FOV in turn to allow enough recovery of fluids without an explicit recovery time.

these, IR scheme 1 provides the best fluid suppression, but also comes with an arterial signal loss in the inferior FOV, probably due to the inflow of not fully recovered blood signal from the superior FOV. On the other hand, IR scheme 2 provides a reasonable trade-off between fluids suppression (dashed arrows, dashed boxes) and arterial signal (solid arrows) by introducing an explicit TI with the expense of a longer scan time.

**Discussion/Conclusion:** In this work, we demonstrated that the proposed IR schemes are feasible for SLINCY, which successfully suppressed the fluids. The extra time for IR is dramatically reduced by exploiting the fact that only a part of the entire volume is acquired with SLINCY at each acquisition step.

- References:** [1] Liu et al., JMRI 1998;8:903. [2] Ruppert et al., 11<sup>th</sup> ISMRM, p.208, 2003. [3] Kwon et al., 20<sup>th</sup> ISMRM, p.3898, 2012. [4] Bangerter et al., JMRI 2006;24:1426. [5] Brittain et al., MRM 1995;33:689. [6] Slavin et al., Radiology 2001;219:258.